In vivo multi-scale evaluation of brightening product efficacy on hyperpigmented spots in high phototype skin

Nastassia Pricoupenko* [1], Randa Jdid[1], Colombe Lopez[2], Clothilde Raoux[2], Gabriel Cazorla[1], Julie Latreille[1], Nada André[1], Youcef Ben Khalifa[1]

[1]Innovation Research & Development, CHANEL Fragrances & Beauty, Pantin, [2]Application Departement, DAMAE Medical, Paris, France

1. Introduction

Hyperpigmentation disorders affect individuals across all skin phototypes. Several forms of hyperpigmented lesions have been identified, including post-inflammatory hyperpigmentation (PIH), melasma, and age spots (lentigines). Due to their higher melanin content, darker skin types are naturally more protected against UV radiation [1], resulting in a lower prevalence of lentigines. However, they are more susceptible to other forms of hyperpigmentation, such as melasma or PIH, often triggered by acne or other inflammatory conditions [2]. These forms of hyperpigmentation tend to be more frequent, more severe, and longer-lasting in darker phototypes compared to lighter ones [3,4]. Consequently, they can persist for months or even years [5], significantly affecting quality of life and contributing to psychosocial distress [6]. Despite their prevalence and impact, hyperpigmented lesions in higher phototypes remain under-characterized, especially in terms of architectural structure and melanin content as well as treatment responsiveness at the microscopic level. In this study, we leverage the non-invasive LC-OCT imaging technique to investigate PIH spots and adjacent skin in three dimensions on high-phototype skin. Thanks to this advanced technique we can visualize skin microarchitecture and assess melanin distribution and density within the epidermis [9-11].

This study aims to characterize hyperpigmented lesions and evaluate the efficacy of a brightening product on high-phototype skin, using both clinical assessments and cutting-edge instrumental techniques at macroscopic and microscopic scales.

2. Materials and Methods

2.1. Study design

A panel of 22 women aged 20 to 49 years (mean age of 33 years) completed the study, the majority presenting with phototype V skin. A total of 60 facial post-inflammatory hyperpigmented (PIH) spots were analyzed, including 45 on phototype V skin. The spots were located

on the forehead (n = 31) and cheeks (n = 29). The study was conducted in Pantin, France, from September 19th, 2023, to December 8th, 2023. Exclusion criteria comprised pregnancy or lactation, non-compliance with cosmetic usage instructions, use of anti-aging or depigmenting agents, exfoliating products or scrubs, a history of aesthetic procedures, and the presence of systemic or dermatological conditions. The investigational brightening product was applied twice daily following a standardized massage protocol. Hyperpigmented spots and adjacent perilesional skin (ref zone) were selected for evaluation at three time points: baseline (T0), after 1 month of product application (T1), and after 2 months (T2).
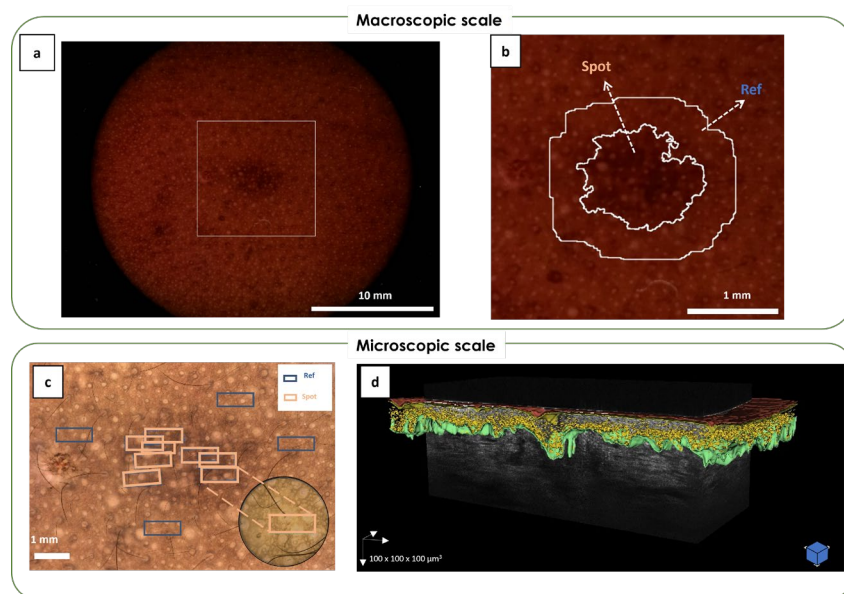

Figure 1 –Spot characterization at macroscopic and microscopic scales (a,b) Cross-polarized images with spot segmentation: (a) original spot image before analysis. The white rectangle indicates the area shown in (b) and (b) cropped image, with spot segmentation highlighting the ref zone and the spot zone (c) Dermoscopic image of the spot with colored rectangles indicating LC-OCT 3D acquisition locations acquisitions : orange for the spot zone and blue for the ref zone. The bottom-right inset shows the macroscopic image integrated into the LC-OCT probe, co-localized with the dermoscopic image. (d) 3D reconstruction of the acquisition location showed in the inset of (c), highlighting skin surface (red), the dermo-epidermal junction (green), and melanin segmentation (yellow).

2.2. Data analysis

Clinical evaluations Evaluations of hyperpigmentated spots improvements were performed on facial photographs under controlled conditions by a trained dermatologist, on 52 hyperpigmented spots chosen on photographs.

Cross-polarized images analysis A semi-automatic segmentation algorithm combining thresholding, morphological operations, distance transformation and watershed algorithm was used to segment the hyperpigmented zone from cross polarized images, acquired with Skin-Cam probe (Newtone Technology, Lyon, France). A reference zone (perilesional skin) was defined as the area within a 100-pixel margin surrounding the segmented spot (**Figure 1 a,b**). At each time point, several colorimetric parameters were measured in both the spot and ref

zones : L* luminance, a* and b* for the color channels green-red and blue-yellow respectively. In addition, the spot area in cm² and spot visibility were quantified. Spot visibility $\Delta E76$ (color distance between spot and ref area) was calculated using the following formula :

$$\Delta E76 = \sqrt{(L_{Ref} - L_{Spot})^2 + (a_{Ref} - a_{Spot})^2 + (b_{Ref} - b_{Spot})^2}$$

LC-OCT acquisitions analysis We used line-field confocal optical coherence tomography (LC-OCT; DAMAE Medical, Paris, France), a non-invasive imaging technique to generate high-resolution cross-sectional, horizontal, and 3D image stacks of the skin. The system provides stacks with a penetration depth of 500 μm, axial resolution of 1.1 μm, and lateral resolution of 1.3 μm. It includes a color macroscopic imaging modality with a 2.5 mm diameter field of view integrated into the probe. An additional videodermoscope enables real-time visualization of probe positioning on dermoscopic images, enabling precise mapping and allowing micrometer-level repositioning after 1 month and 2-month product use. For hyperpigmented zones, 4 to 10 LC-OCT 3D acquisitions were performed at each time point, on both the spot and surrounding skin (**Figure 1 c,d**). Acquisitions with motion artifacts were excluded.
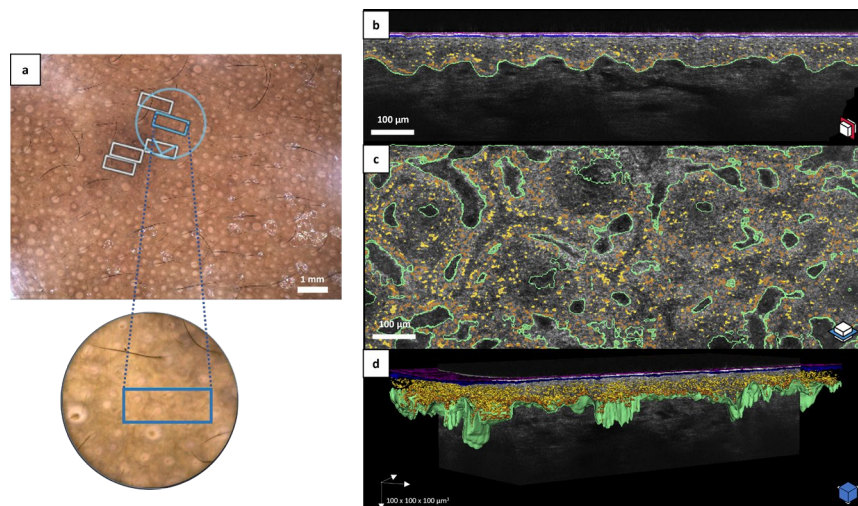

Figure 2 – Skin layers and melanin segmentation from LC-OCT acquisitions **(a)** Dermoscopic image of the PIH spot, indicating LC-OCT 3D acquisition locations. The bottom-right inset shows the macroscopic image integrated into the LC-OCT probe **(b)** Vertical and **(c)** horizontal LC-OCT images, and **(d)** 3D reconstruction highlighting skin surface (pink), stratum corneum end (blue), the dermo-epidermal junction (green) and segmented melanin in the suprabasal layers (yellow) and in the basal layer (orange).

o *Skin layers segmentation and quantification* A validated skin layer segmentation algorithm was used to segment the skin layers : the surface, stratum corneum end, and dermal–epidermal junction (DEJ) [9] (**Figure 2**). The thickness and undulation of each layer were extracted, excluding hair follicles. The percentage of DEJ undulation was calculated using the following formula: $\%U_{DEJ} = ((S_{DEJ}/ S_{ROI}) - 1) \times 100$, where S_{DEJ} represents the surface area of the dermo–epidermal interface, and S_{ROI} is the total horizontal area of the LC-OCT image excluding hair follicles.

○ ***Melanin segmentation and quantification*** Melanin segmentation was performed using an AI algorithm developed by DAMAE Medical [8]. Surfacic melanin density (number of melanin pixels divided by S_{ROI}) was calculated for the entire epidermis, as well as for the basal layer (15 µm above the DEJ), and suprabasal layers (**Figure 2 b-d**). The melanin distribution profile was calculated across 20 layers from stratum corneum end surface to DEJ and averaged by spot and time point.

Statistical analysis Several statistical tests were performed using Python's statistical tools (using the scipy library). The normality of the distribution was tested with a Shapiro test. For normally distributed data, Student's *t*-test was used to evaluate differences between group means (results shown in green). When normality was not confirmed, the non-parametric Wilcoxon signed-rank test was applied (results shown in blue). Statistical significance is indicated as follows: n.s. (not significant) for $p > 0.05$; * for $p < 0.05$; ** for $p < 0.01$; and *** for $p < 0.001$.

3. Results

3.1. Characterization of hyperpigmented PIH spots

At baseline (T0), before treatment, analysis of cross-polarized images revealed that hyperpigmented PIH spots exhibited significantly lower values of luminance L* (-40%, p=8.10^{-12}), a* (-10 %, p=4.10^{-10}) and b* (-31%, p=1.10^{-27}) compared to the surrounding skin (**Figure 3 a,b**). The color contrast between the spots and adjacent skin, quantified by the $\Delta E76$ metric, was measured at 8.6, indicating a high level of spot visibility.
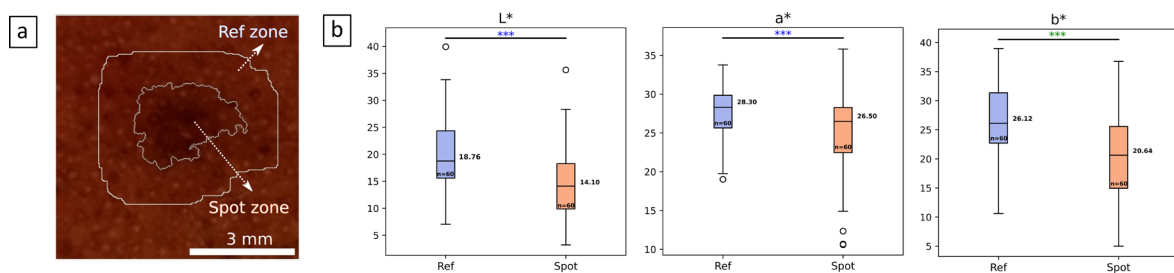

Figure 3 - Characterization of hyperpigmented spot compared to adjacent skin at the macroscopic scale (a) Cross polarized image of a PIH spot and overlaid spot segmentation contours in white. (b) From left to right: mean luminance L*, mean a* color channels green-red and mean b* color channels blue-yellow in PIH spot in orange compared to surrounding skin, ref zone in blue.

The LC-OCT technique enabled detailed characterization of PIH spots at the microscopic level, both in terms of skin architecture and melanin content (**Figure 4 a,b**). Compared to surrounding skin, these areas exhibited a significantly thicker epidermis (+14%, p=5.10^{-11}), an increased DEJ undulation (+23%, p=3.10^{-7}) as well as an increased surfacic melanin density (+7,6%, p=0.0002) (**Figure 4 c**). As we observed a difference in the repartition of melanin in the epidermis between hyperpigmented spots and adjacent skin (**Figure 5 a**), we further analyzed the content of melanin specifically in the basal and the suprabasal layers. Interestingly,

PIH spots exhibited a significant increase in surfacic melanin density within the suprabasal layers of the epidermis (+30%, $p=3.10^{-11}$), highlighting a key feature of these spots. However a reduced melanin content is found in the epidermis basal layer (-15%, $p=0.03$) (**Figure 5 b**). This unexpected result [10] may be attributed to the model's limited ability to detect melanin in deeper epidermal layers when the total epidermal thickness exceeds 80 µm. Indeed PIH often presents with a thickened epidermis, unlike other pigmented lesions the model was trained on. This could explain the less pronounced melanin detection in the basal layer of PIH lesions compared to surrounding skin. Future work will focus on refining the model to address these variations. Due to this limitation, basal layer melanin content will not be used to evaluate product efficacy.
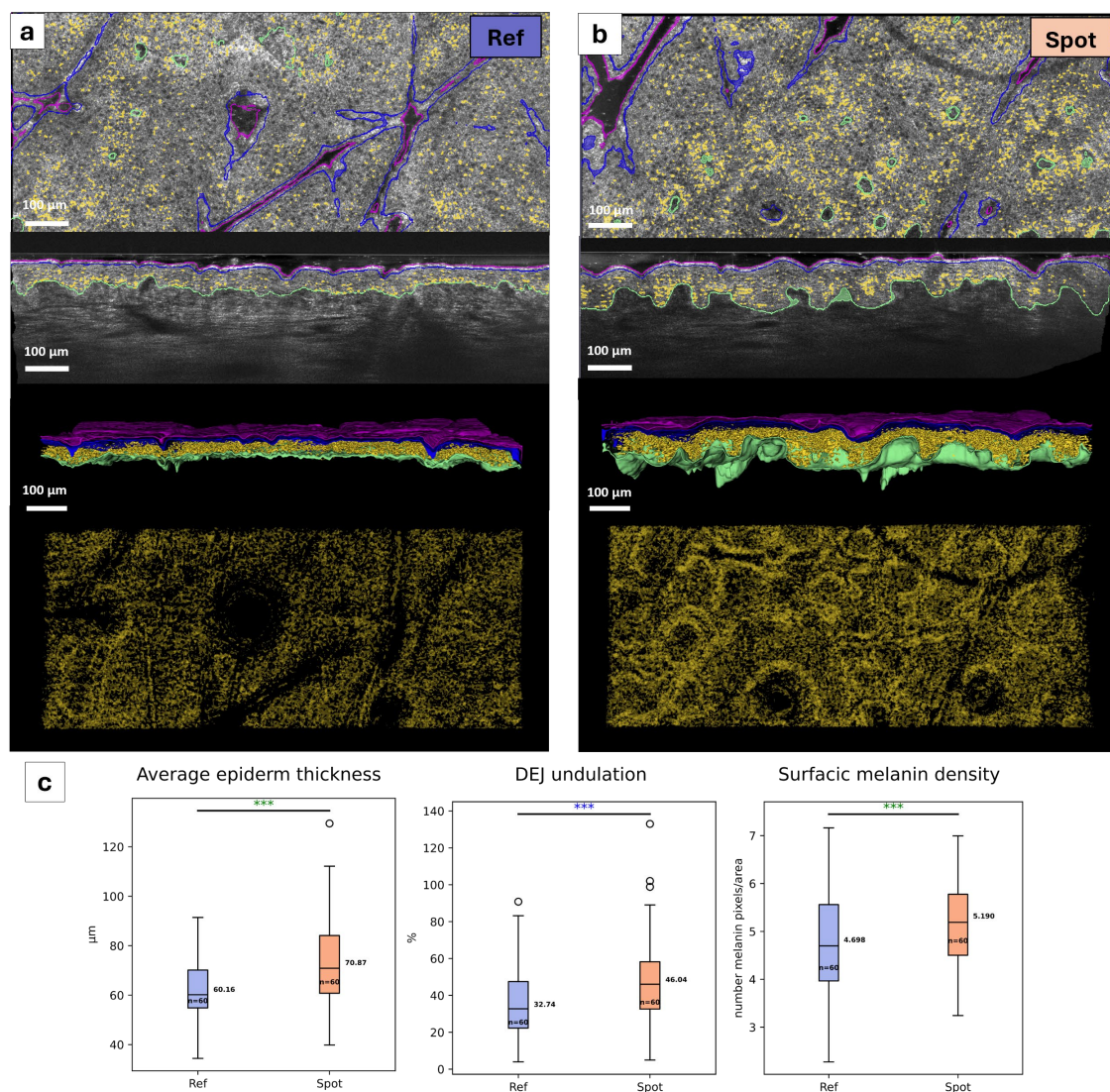

Figure 4. Characterization of PIH spot compared to adjacent skin at the microscopic scale (a,b) From top to bottom: horizontal and vertical LC-OCT images, 3D reconstruction highlighting skin surface (pink), stratum corneum end (blue), the dermo-epidermal junction (green) and segmented melanin (yellow), and horizontal image of projected segmented melanin for Ref zone (non-lesional skin) (a) and for the spot zone (b) shown in Figure 3 a. (c) From left to right, average epidermis thickness, DEJ undulation and surfacic melanin density in epidermis.
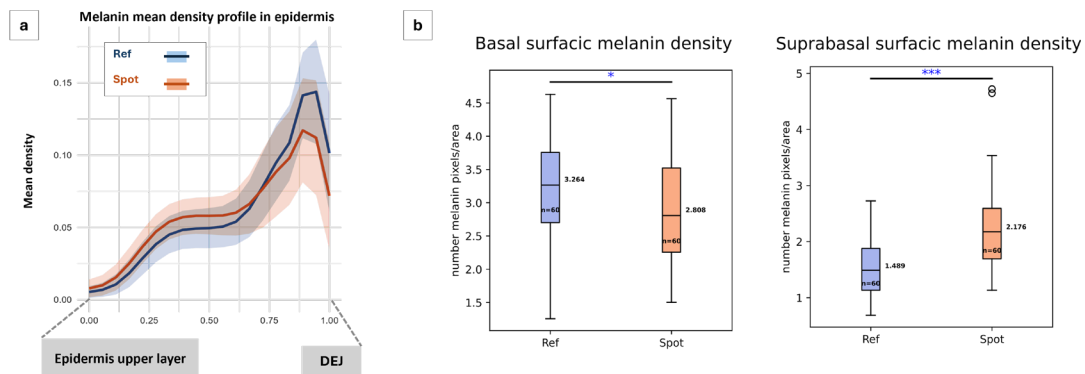
Figure 5. Epidermal melanin distribution in PIH spots compared to adjacent skin (a) Melanin density profiles in epidermis, plotted along normalized distances from the stratum corneum end to the dermo-epidermal junction (DEJ), for PIH spots (orange) and surrounding skin (blue). Solid lines represent the mean values; shaded areas indicate standard deviations. (b) Surface melanin density in the basal (left) and suprabasal (right) epidermal layers, in PIH spots (orange) and surrounding skin (blue).

3.2. Evaluation of efficacy of brightening product at the macroscopic level

Clinical evaluation on facial photographs (n = 52 spots) revealed visible improvement in 39 spots after 1 month of treatment, and in 47 spots after 2 months. Instrumental assessment of macroscopic efficacy was conducted on cross-polarized images of 53 hyperpigmented PIH spots and their adjacent skin, captured at baseline (T0), after 1 month (T1), and after 2 months (T2) of daily application of the brightening product. For 7 spots, efficacy could not be assessed due to insufficient image quality at either T1 or T2.
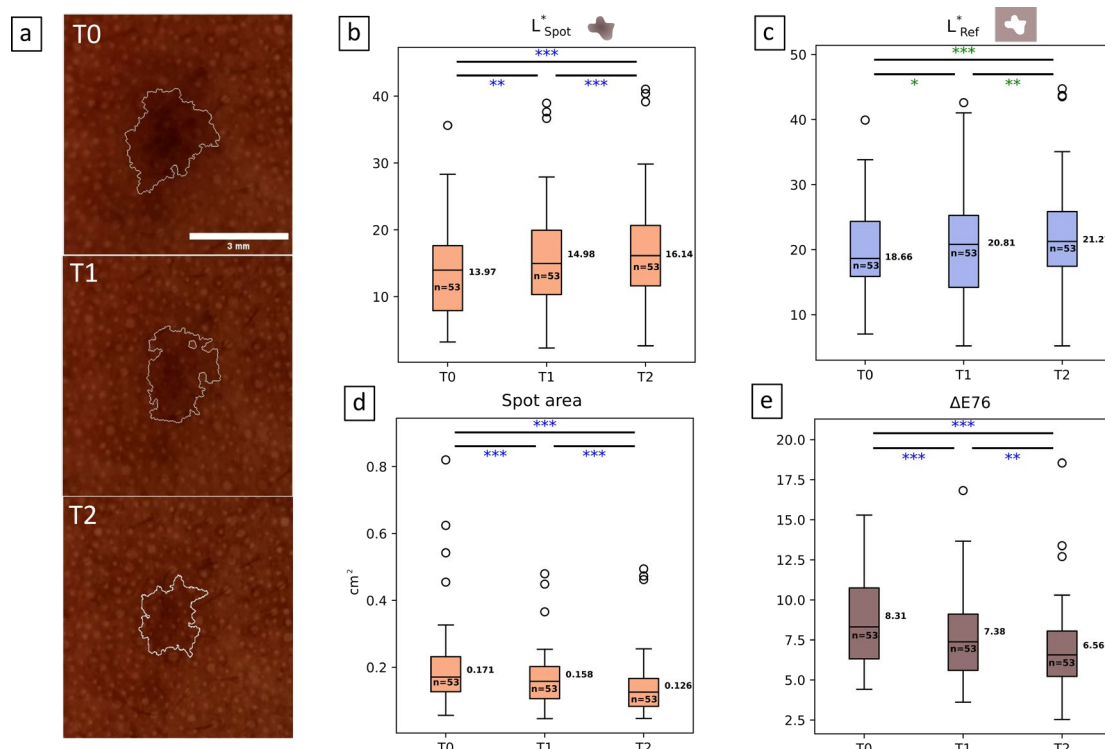

Figure 6. Evaluation of efficacy of brightening product at the macroscopic level (a) From top to bottom: cross polarized images of an hyperpigmented PIH spot at baseline, after 1 month product use (T1) and after 2 months (T2). (b-c) Evolution of luminance L* for spot zone (b) and ref zone (c). (d) Evolution of spot area and (e) evolution of spot visibility during the 2-month study for n=53 hyperpigmented spot zones.

Given the strong correlations between L* and both a* and b* values (> 0.85), luminance (L*) was selected as the primary metric for evaluating colorimetric changes in both the spot and adjacent skin. A significant brightening effect was observed after 1 month, with further improvement after 2 months of product use. Specifically, luminance increased by 19% in the hyperpigmented spots (p=4.10^{-7}) and by 8,6% in the ref zone (p=7.10^{-5}) (**Figure 6 a,b,c**). In parallel, a significant reduction in spot size was measured, with a 24% decrease in surface area after 2 months (p=2.10^{-7}) (**Figure 6 d**). Moreover, spot visibility quantified by the color contrast $\Delta E76$ between spot and adjacent skin was reduced by 16% (p=3.10^{-6}) over the same period (**Figure 6 e**).

3.3. Evaluation of efficacy of brightening product at the microscopic level

The efficacy of the product at the microscopic level was evaluated using LC-OCT acquisitions performed within the PIH spots and adjacent skin at baseline (T0), 1 month (T1), and 2 months (T2) of daily product application (**Figure 7**).
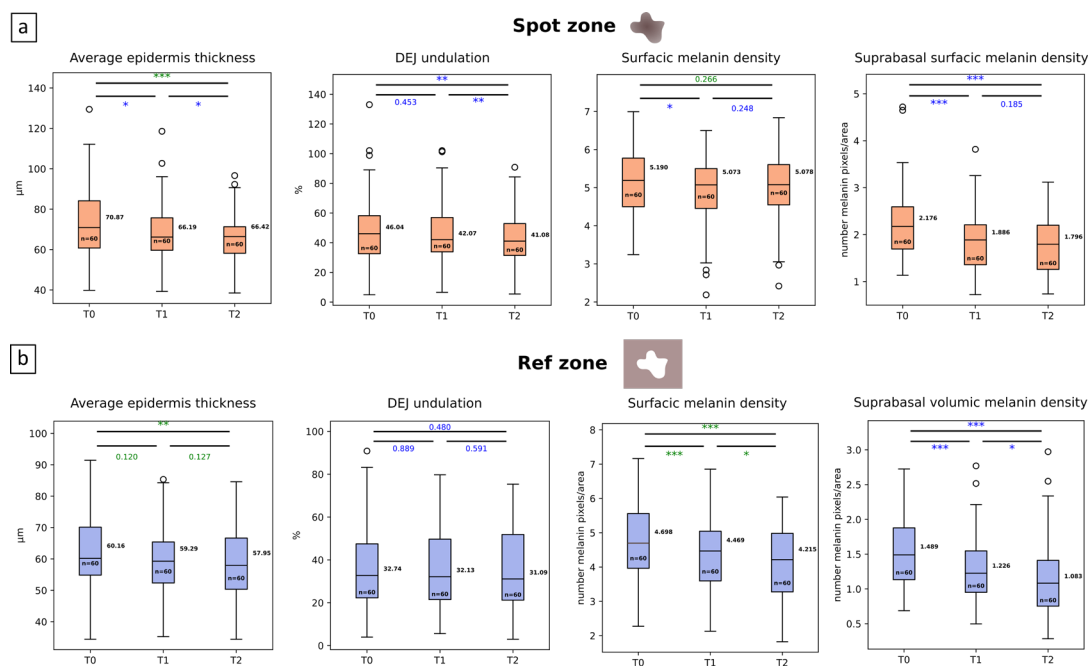

Figure 7. Evaluation of efficacy of brightening product at the microscopic level. (a,b) from left to right: evolution of average epiderm thickness, DEJ undulation, surfacic melanin density and suprabasal volumic melanin density for n=60 pigmented spot zones evaluated at baseline (T0), after 1 month product use (T1) and after 2 months (T2) for the spot zone (a) and the surrounding area (b).

Significant morphological changes were observed over time. Epidermal thickness was reduced by 6,2% within the spot (*p* = 0.0003) and by 7,2% in the surrounding skin (*p* = 0.0025) between T0 and T2 (**Figure 7**). In parallel, a 10% decrease in DEJ undulation was observed within the spots (*p* = 0.007), while no significant change was found in the adjacent skin (*p* = 0.48), indicating a localized architectural remodeling effect in spots. Regarding the pigmentation, a reduction in the melanin surfacic density of the suprabasal layers was observed between T0 and

T2 (-17%, p=0.0002). Overall melanin surfacic density showed a significant decrease after 1 month (-3,0%, p = 0.024) and a non-significant trend between T0 and T2 (-1,7%, p = 0.27). We observed higher efficacy in the surrounding skin than in the spot, with a reduction in the melanin surfacic density within the suprabasal layers (-32%, p =2.10^{-6}) and in the overall melanin surfacic density (-7,6%, p =6.10^{-7}).

4. Discussion

This study presents a comprehensive, multi-scale in vivo characterization of post-inflammatory hyperpigmentation (PIH) in phototype V–VI skin, spanning from macroscopic observations to microscopic analyses. To our knowledge, this is the first investigation to provide such an in-depth, multi-level assessment of PIH in darker skin types.

At the microscopic level, our findings align with those of Hokazaki et al., who previously described PIH-associated structural changes in phototype III Asiatic skins [11]. Specifically, we observed a localized modification of skin architecture within PIH spots, including increased epidermal thickness and a more undulated DEJ compared to adjacent non-lesional skin. In addition, the hyperpigmented spots exhibited a higher melanin surfacic density, consistent with the lower luminance found in these areas and the histological features of PIH reported in the literature [12-13]. Beyond melanin quantification, this study also investigated its spatial distribution. Notably, we identified a marked accumulation of melanin within the suprabasal layers of the epidermis in the hyperpigmented spots, compared to the adjacent non-lesional skin.
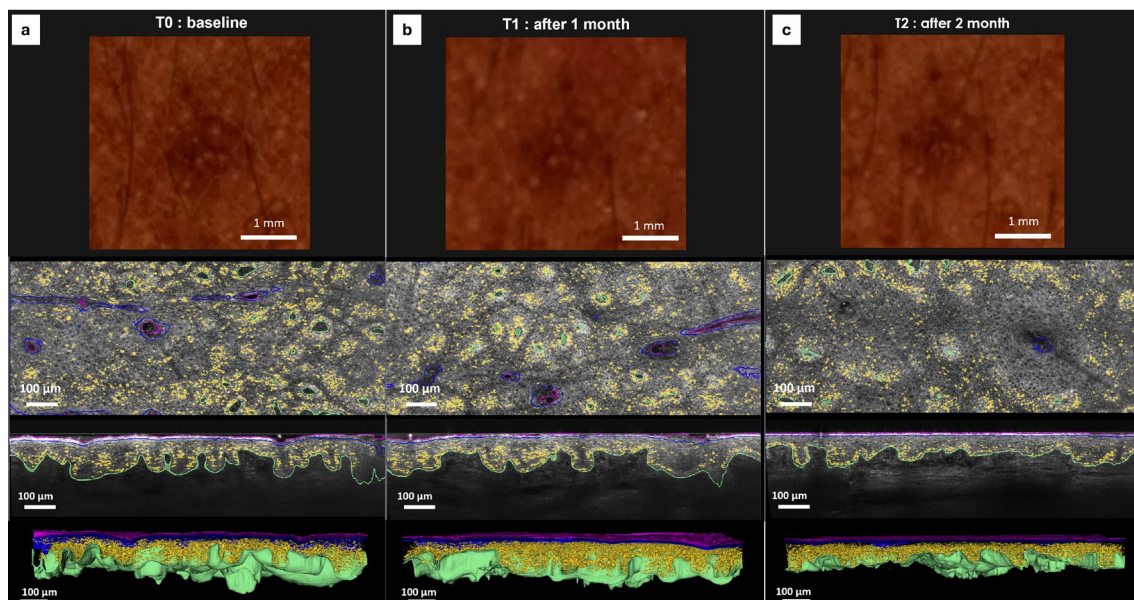

Figure 8. Representative images illustrating the effect of the brightening product on a PIH spot at the macroscopic and microscopic levels. From top to bottom, cross-polarized image of the spot, horizontal and vertical LC-OCT images, and 3D reconstruction highlighting skin surface (pink), stratum corneum end (blue), dermo-epidermal junction (green) and segmented melanin (yellow) at baseline **(a)**, after 1 month **(b)** and after 2 months **(c)**.

For the first time, we also evaluated the in vivo efficacy of a topical brightening product on phototype V–VI skin with PIH spots at both macroscopic and microscopic scales (**Figure 8**).The product evaluated is designed to brighten hyperpigmented lesions as well as the surrounding skin. At the macroscopic level, it significantly reduced spot size, pigmentation intensity, and lesion visibility. While several studies have examined the efficacy of topical brightening products at the macroscopic scale [13-14], few have investigated their impact at the microscopic level [10,15]. After 2 months of application, we observed a reduction in epidermal thickness in both PIH spots and adjacent areas, as well as a significant decrease in DEJ undulation within spots, suggesting an architectural improvement of PIH. Surfacic melanin density decreased significantly after 1 month in both spots and adjacent skin but the reduction remained significative only for adjacent skin after 2 months. Remarkably, surfacic melanin density in epidermis suprabasal layers were reduced in both spots and surrounding skin. Surprisingly, although macroscopic evaluations demonstrated greater improvement within the spots, microscopic analyses indicated a more substantial effect in the surrounding skin. This apparent inconsistency may be explained by a thinner epidermis within the lesion after 2 months compared to baseline. As the detection algorithm was not specifically trained on skin with markedly thick epidermis, its performance appears more accurate on skin with thinner epidermis. This may have resulted in an underestimation of melanin reduction within the spots. The observed brightening effects of the product can be attributed to the unique combination of Ylang Ylang and niacinamide, which has demonstrated notable efficacy in reducing melanin content on a patented bioprinting technology 3D in vitro skin model (article in preparation). Ylang Ylang inhibits melanogenesis [15] while niacinamide reduces suprabasal melanin content by inhibiting melanosome transfer from melanocytes to keratinocytes [16].

In summary, our study demonstrates the efficacy of a topical brightening product in enhancing both the clinical appearance and microscopic features of PIH, through modulation of skin architecture, as well as melanin distribution and content. These findings contribute to a better understanding of hyperpigmentation in darker skin types and highlight the importance of multiscale assessment in evaluating treatment outcomes for PIH.

5. Conclusion

By combining LC-OCT with traditional colorimetric analysis, this study is the first to investigate hyperpigmented spots in phototypes V-VI in a non-invasive way from microscopic to macroscopic scales. PIH spots showed significant architectural and pigmentary alterations, which were effectively improved by the brightening product. This novel approach enabled accurate monitoring of pigmented spots, paving the way for deeper characterization of pigmentation disorders and their treatments.

[1] M. Brenner and V. J. Hearing, "The Protective Role of Melanin Against UV Damage in Human Skin†," *Photochem Photobiol*, vol. 84, no. 3, pp. 539–549, May 2008, doi: 10.1111/J.1751-1097.2007.00226.X.

[2] N. Elbuluk *et al.*, "The Pathogenesis and Management of Acne-Induced Post-inflammatory Hyperpigmentation," *Am J Clin Dermatol*, vol. 22, no. 6, pp. 829–836, Nov. 2021, doi: 10.1007/S40257-021-00633-4/METRICS.

[3] E. C. Davis and V. D. Callender, "Postinflammatory Hyperpigmentation: A Review of the Epidemiology, Clinical Features, and Treatment Options in Skin of Color," *J Clin Aesthet Dermatol*, vol. 3, no. 7, p. 20, Aug. 2010.

[4] E. Markiewicz, N. Karaman-Jurukovska, T. Mammone, and O. C. Idowu, "Post-Inflammatory Hyperpigmentation in Dark Skin: Molecular Mechanism and Skincare Implications," *Clin Cosmet Investig Dermatol*, vol. 15, pp. 2555–2565, 2022, doi: 10.2147/CCID.S385162.

[5] F. Abad-Casintahan *et al.*, "Frequency and characteristics of acne-related post-inflammatory hyperpigmentation," *J Dermatol*, vol. 43, no. 7, pp. 826–828, Jul. 2016, doi: 10.1111/1346-8138.13263.

[6] K. Darji, R. Varade, D. West, E. S. Armbrecht, and M. A. Guo, "Psychosocial Impact of Postinflammatory Hyperpigmentation in Patients with Acne Vulgaris," *J Clin Aesthet Dermatol*, vol. 10, no. 5, p. 18, May 2017.

[7] J. Ogien, O. Levecq, H. Azimani, and A. Dubois, "Dual-mode line-field confocal optical coherence tomography for ultrahigh-resolution vertical and horizontal section imaging of human skin in vivo," *Biomed Opt Express*, vol. 11, no. 3, p. 1327, Mar. 2020, doi: 10.1364/BOE.385303.

[8] R. Jdid *et al.*, "Skin dark spot mapping and evaluation of brightening product efficacy using Line-field Confocal Optical Coherence Tomography (LC-OCT)," *Skin Research and Technology*, vol. 30, no. 2, Feb. 2024, doi: 10.1111/SRT.13623.

[9] J. Ogien, C. Tavernier, S. Fischman, and A. Dubois, "Line-field confocal optical coherence tomography (LC-OCT): principles and practical use," *Italian Journal of Dermatology and Venereology*, vol. 158, no. 3, pp. 171–179, Jun. 2023, doi: 10.23736/S2784-8671.23.07613-2,.

[10] J. Y. Park *et al.*, "Two histopathological patterns of postinflammatory hyperpigmentation: epidermal and dermal," *J Cutan Pathol*, vol. 44, no. 2, pp. 118–124, Feb. 2017, doi: 10.1111/CUP.12849.

[11] T. Hakozaki *et al.*, "Morphological and transcriptional evaluation of multiple facial cutaneous hyperpigmented spots," *Skin Health and Disease*, vol. 2, no. 2, Jun. 2022, doi: 10.1002/SKI2.96.

[12] E. T. Makino, P. Huang, T. Cheng, S. F. Acevedo, C. de Oliveira, and R. C. Mehta, "12-Week, Single-Center Study of a Targeted Pigment-Correcting Dark Spot Treatment for Post-Inflammatory Hyperpigmentation and Solar Lentigines," *Clin Cosmet Investig Dermatol*, vol. 16, pp. 2677–2686, Sep. 2023, doi: 10.2147/CCID.S427956.

[13] N. J. Lowe, D. Rizk, P. Grimes, M. Billips, and S. Pincus, "Azelaic acid 20% cream in the treatment of facial hyperpigmentation in darker-skinned patients," *Clin Ther*, vol. 20, no. 5, pp. 945–959, 1998, doi: 10.1016/S0149-2918(98)80076-3.

[14] J. P. Castanedo-Cazares *et al.*, "Topical niacinamide 4% and desonide 0.05% for treatment of axillary hyperpigmentation: A randomized, double-blind, placebo-controlled study," *Clin Cosmet Investig Dermatol*, vol. 6, pp. 29–36, Jan. 2013, doi: 10.2147/CCID.S39246.

[15] T. Matsumoto *et al.*, "Lignan dicarboxylates and terpenoids from the flower buds of cananga odorata and their inhibitory effects on melanogenesis," *J Nat Prod*, vol. 77, no. 4, pp. 990–999, Apr. 2014, doi: 10.1021/NP401091F/SUPPL_FILE/NP401091F_SI_001.PDF.

[16] T. Hakozaki *et al.*, "The effect of niacinamide on reducing cutaneous pigmentation and suppression of melanosome transfer," *Br J Dermatol*, vol. 147, no. 1, pp. 20–31, 2002, doi: 10.1046/J.1365-2133.2002.04834.X.